

# Envelope Spectrum Analysis for Rolling Element Bearing Faults Diagnosis by Using Kurtogram and Spectral Kurtosis for Band Selection

Vivekkumar\*, Dr.Premamamd S Chauhan\*\*, Jitendra Dubey\*\*\*

\*Resaech Scholar Department of Mechanical Engineering, IPS College of Technology & Management, Shivpuri Link Road,Gwalior(MP),India, vivek161093@gmail.com

\*\*Principal, Department of Mechanical Engineering, IPS College of Technology & Management, Shivpuri Link Road,Gwalior(MP),India, qforquaid@gmail.com

\*\*\*Director, UdayEductaionAcademy,Gwalior(MP),India , jitenda.dubey@gmail.com

---

## ABSTRACT

Due to geometrical defects, surface irregularities during manufacturing, defective bearing used, and error in the related part, a rolling-element bearing produces a complex vibration. Background noise normally masks these acceleration signals. When the raw vibration signal is surrounded by heavy noise, this research paper shows how to isolate the fault function frequency by using kurtosis, spectral kurtosis, and a bandpass filter before the envelope spectrum. Furthermore, this report has revealed several methods for extracting various frequency spectrum characteristics. The vibration signal case analysis was addressed in this article, and the vibration signal was submerged in strong background noise. The envelope spectrum analysis fails to separate the fault mechanism from this signal, necessitating the use of a more sophisticated approach to resolving this problem. Until enveloping, many researchers used the de-noising method as a pre-filter. De-noising also has certain disadvantages, such as the lack of initial elements. The efficiency of signal processing algorithms is harmed by noise. To solve these flaws, kurtosis, spectral kurtosis, and a bandpass filter are applied before the envelope spectrum. These frequency spectrum properties benefit carrying health more effectively. Envelope analysis is a useful vibration analysis technique for bearing diagnostics. The frequency-domain characteristics, which allow a fast assessment of a machine's health without comprehensive diagnostics. Using envelope analysis on the modulated signal, the intermittent impacts of a defected bearing were recorded. It is still rational when the vibration signal is low in energy and 'embedded' within additional vibration from the relevant component.

**Keywords: Frequency domain, spectral kurtosis, Rolling element bearing, Fault Investigation.**

\*\*\*\*\*

## 1. INTRODUCTION

REBs (rolling element bearings) are used in a variety of industrial applications, and their failure can lead to machinery breakdown [1][2]. To prevent these types of bearing failures, fault inspection is required [2][3]. Holding vibration data provides a wealth of knowledge about faults and their locations [4]. In rolling component bearings, vibration analysis is often used to locate localized defect. The periodic force impacts in the presence

of a defect are caused by impulsivity at a fixed frequency, which is measured using the shaft speed, sampling frequency, and bearing geometry[2][4][3]. As a result, intermittent impulses are a critical state predictor of REBs, and the bearing characteristic frequencies (BCFs) are usually classified by assuming the outer race is stationary in most cases[4][5] [7].

This paper explains how to do fault analysis on a rolling part bearing. In addition, the noisy vibration signal from the machine's related part is

studied in this article. This paper's approach shows how to use envelope spectrum analysis in addition to spectral kurtosis. Localized defects appear in bearings in a variety of places, including the inner race (IR), the outer race (OR), the ball, and the cage [8]. Figure 1 shows a system schematic of inner race defects (1).

Critical frequencies vary depending on the defect position: The first is the ball pass frequency outer race (BPFO), which has the signature frequencies as follows:

$$BPFO = \left\{ \frac{N}{2} \left[ f_i \left( 1 - \frac{d \cos \alpha}{PD} \right) \right] \right\}$$

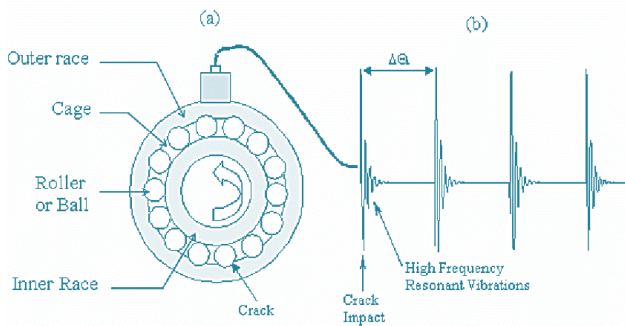


Fig. 1. Bearing with outer race affected by crack. (a) Bearing (b) Time domain signal

Ball pass frequency inner race (BPFI), fundamental train frequency (FTF), and ball spin frequency (BSF) are the other important frequencies that express different defect positions. The following are the formulae for certain signature frequencies [9]:

$$BPFI = \left\{ \frac{N}{2} \left[ f_i \left( 1 + \frac{d \cos \alpha}{PD} \right) \right] \right\} \quad (2)$$

$$FTF = f_g = \frac{1}{2} \left[ f_i \left( 1 - \frac{d \cos \alpha}{PD} \right) \right] \quad (3)$$

$$BSF = f_r = \frac{D_p}{2d} (f_i) \left[ 1 - \left( \frac{d \cos \alpha}{PD} \right)^2 \right] \quad (4)$$

Where the number of rolling element N, pitch diameter of bearing PD, diameter of ball d, angle of contact  $\alpha$  and the shaft speed is denoted by  $f_i$ .

## 2. ENVELOPE SPECTRUM ANALYSIS AND SPECTRAL KURTOSIS

### 2.1 Envelope Spectrum Analysis

Since the signals of a faulty system are modulated by defect characteristics, a demodulation investigation is expected. Envelope analysis, for example, may provide a quantitative analysis of the signals received. Envelope analysis, also known as high-frequency resonance analysis, is a signal-processing technique that can be considered as a prevalent and accurate classification for defect detection in rotating machine bearings [10].

In general, envelope spectrum analysis is performed in three steps: first, the initial vibration data is band-pass filtered; second, the time domain signal is enveloped by wrapping the base component over the uppermost part of the signal accompanied by Hilbert-Huang transform (HHT); and third, it is updated by using fast Fourier transform (FFT). Finally, the envelope spectrum obtained from vibration data includes specific peak amplitude information. The FFT domain does not explicitly show these peak amplitudes [1][10][11].

### 2.2 Spectral Kurtosis

Kurtosis is described as the fourth normalized central moment used to determine if the distribution peak is higher or lower [12]. Dwyer (1983) proposed a frequency domain kurtosis (FDK) method, which is the advancement of time-domain spectral kurtosis (SK). The frequency-domain kurtosis is interpreted as the ratio the fourth-order central moment of the short term Fourier transforms divided by the square of the second-order central moment of the short term Fourier transforms (STFT) (Dwyer 1984). Mathematically

$$x_{FDK}(f) = \frac{E\{[x(q, f_p)]^4\}}{E\{[x(q, f)]^2\}^2} \quad (5)$$

Where,

$$x(q, f) = \sqrt{\frac{h}{m}} \sum_{i=0}^{m-1} w_i x(i, q) \exp(-jfp i) \quad (6)$$

also,  

$$x(i, q,) = x[i + (q - 1)m]n] \quad (7)$$

Where,

$h$  = the period among succeeding measurements of the method,  $w_i = 1$ ,  $f = 2\pi/m$ ,  $q = 1, 2 \dots n$ ,  $i = p = 0, 1, 2, \dots m$ , and  $j = \sqrt{-1}$ , and  $x(i, q,) =$  signal input.

The most basic application of the spectral kurtosis technique is to use the kurtosis at a certain frequency to detect the appearance of non-Gaussian elements, as well as the frequency bands in which such non-Gaussian elements occur. A signal's spectral kurtosis is defined as the kurtosis of a single frequency variable. Signal decomposition of a time waveform in the time domain yields spectral kurtosis, with the magnitude of kurtosis in the frequency group defined locally. [11][13]. The spectral kurtosis signal  $x(t)$ , The fourth-order normalized cumulate is known as Spectral kurtosis  $x_{SK}(f)$  and calculated by equation (8) :

$$x_{SK}(f) = \frac{\langle |H(t, f)|^4 \rangle}{\langle |H(t, f)|^2 \rangle^2} - 2 \quad (8)$$

$$H(t, f) = \int_{-\infty}^{+\infty} x(\tau) w(\tau - t) e^{-j2\pi f \tau} d\tau \quad (9)$$

Where  $H(t, f)$  is the complex envelope function of  $x(t)$  at frequency  $f$  captured utilizing the short term Fourier transforms algorithm [14] suggested the Kurtogram algorithm, which was derived from spectral kurtosis [14]. The Kurtogram algorithm uses a bandpass filter to measure spectral kurtosis for different window sizes. Using the kurtogram's central frequency ( $fc$ ) and bandwidth ( $bw$ ), the signal is bandpass filtered to refine the kurtogram.

### 3. EXPERIMENTAL INVESTIGATION

#### 3.1 Description of test rigs

Case Western Reserve University (CWRU) established the bearing data for the above article [17]. In this experiment, an SKF 6203-2RS JEM deep groove ball bearing was used. For all forms of faults considered, the sampling frequency is set to 12000 Hz. The load ranges from 0 to 3 horsepower, with shaft speeds ranging from 1772 to 1730 revolutions per minute. The laboratory setup used in this study as seen in Fig. (2). In an experimental bearing, electrical discharge machining is used to create artificial defects of different diameters in various positions within the inner and outer races [17].

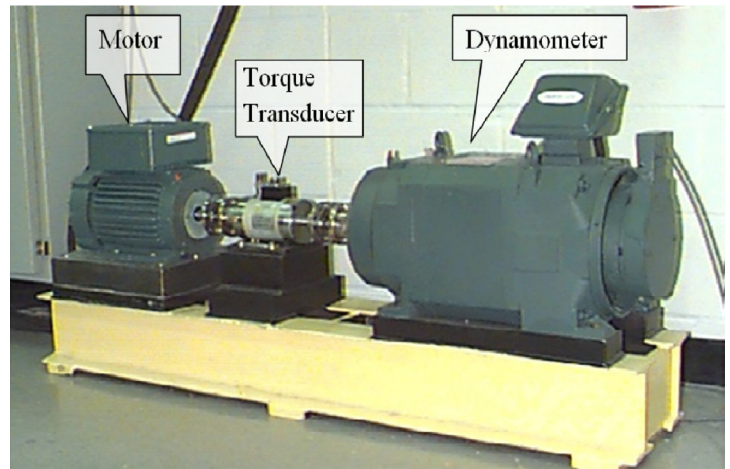
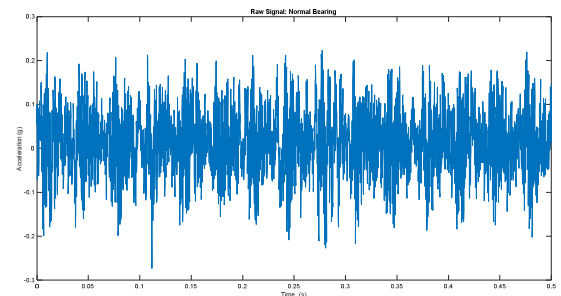
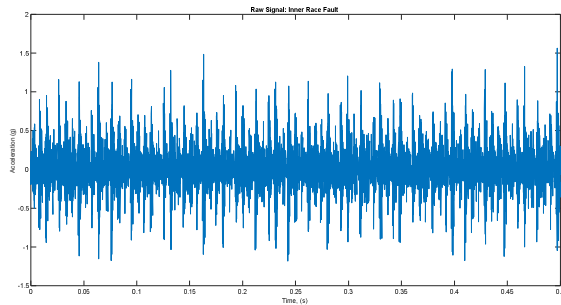


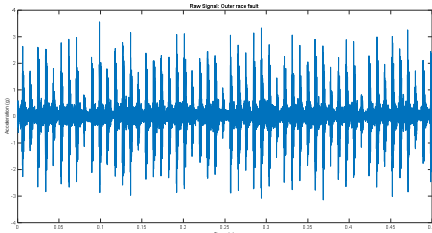
Fig. 2. Experimental setup [17].



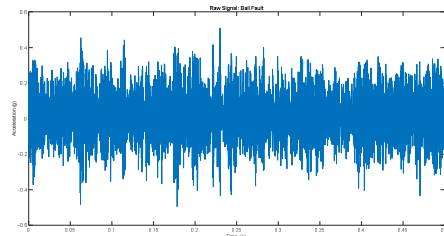
(a) Time-domain raw signal from Normal bearing.



(b)Time-domain raw signal from Inner race fault.



(c)Time-domain raw signal from Outer race fault



(d)Time-domain raw signal from Outer race fault.

**Fig. 3.** Time-domain waveform obtain from test bearing at 1797 rpm (a) Normal bearing (b) Inner race fault (c) Outer race fault and (d) Ball fault

Figure 3 shows four Time Domain waveforms plot of the experimental bearing at 1797 rpm. Time-domain waveform (acceleration vs time) obtain from test bearing at 1797 rpm (a) Normal bearing (b) Inner race fault (c) Outer race fault and (d) Ball fault. The sampling frequency in the experimental investigation are 12000 Hz and for 0.5 seconds plot is mention above in this paper.

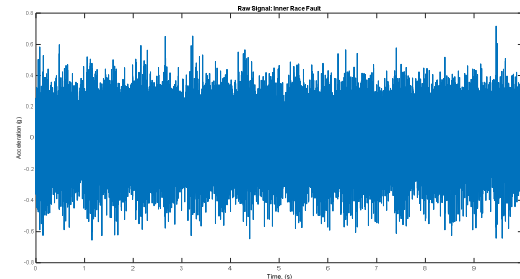
### 3.2 Inner race fault investigation (Instance 1)

**Instance 1:** The first case contains a flaw on the bearing 6203-SKF's inner race. In this experimental investigation, the information about the defect diameter is obtained 0.1778 mm with a depth of 0.2

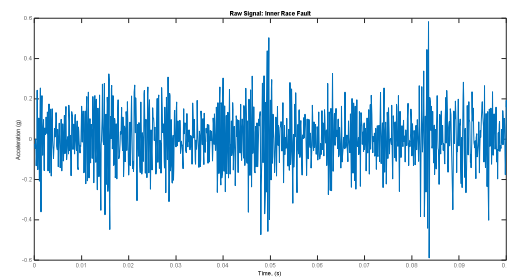
mm in case of inner race and outer race fault type, whereas 0.1 mm depth is measured in case of ball fault. The motor load is set to 0 hp in this experiment and position relative to the load zone in case of outer race defect is centered at 06:00 shown in Table 1 and Table 2 respectively. The envelope analysis is used to find the inner race flaw. The BPF and associated parameters for the 6203-SKF bearing as follows:

$$BPF = \left\{ \frac{N}{2} \left[ f_i \left( 1 + \frac{d \cos \alpha}{PD} \right) \right] \right\}$$

Where the  $N=08$ ,  $PD = 28.49 \text{ mm}$ ,  $d = 6.74 \text{ mm}$ ,  $\alpha = 0 \text{ degree}$ , inside diameter of bearing =  $17 \text{ mm}$ , and outside diameter of bearing =  $40 \text{ mm}$ . The sampling frequency and total data point in the experimental investigation are 12000 Hz and 121535. The shaft frequency  $f_i = 29.95 \text{ Hz}$ . As a result of the aforementioned calculation, the corresponding BPF, according to the bearing's specifications, is 148.1416 Hz.



(a) Time-domain raw signal Inner race fault for 10 seconds



(b)Time-domain raw signal Inner race fault for 0.1 seconds

**Fig. 4.** Time-domain waveform obtain from test bearing at 1797 rpm of Inner race fault (a) for 10 seconds waveform capture (b) for 0.1 seconds waveform capture

Order tracking is a pre-processing technique for reducing the impact of shaft speed changes. However, since the shaft speed is standardized in this experiment, there is no need to complete the order monitoring procedure. In the time domain, Figure 4 depicts the initial inner race fault signature.

From figure 4(b) time-domain signal, show that the initial signal amplitude is modulated at a certain frequency.  $T = 0.00676 \text{ 1/BPFI}$ ,  $\text{BPFI} = 147.93$ . It means that the inner race of the rolling element bearing has a fault.

Recognize the raw data in the frequency domain, and Figure 5 displays the raw signal Inner Race fault envelope signal and the related Inner Race fault envelope spectrum (5)

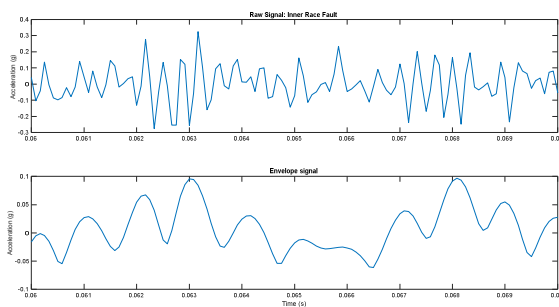


Fig. 5. Envelope signal of raw signal Inner Race fault.

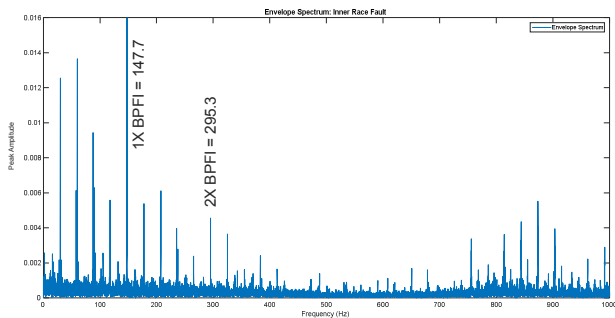


Fig. 6. IRDefect observed in envelope spectrum with BPFI and its harmonics.

Figure 6 shows the following: The various peaks are visible and provide crucial information about the fault type. This diagram shows the frequency values of various peaks as well as their

harmonic multiples. Peaks at frequency 147.7 Hz with frequency harmonics were found to be 295.3 Hz. The determined BPFI 148.1416 agrees with the BPFI found with its harmonics. The frequency 148.1416 Hz is revealed. As a result, the envelope analysis can be used to classify the inner race fault.

**Bearing with outer race fault investigation (Instance 2)**

Instance 2 is an outer track fault investigation involving bearing 6205-SKF with an outer race fault. In this experimental investigation, the information about the defect diameter is obtained 0.1778 mm with a depth of 0.2 mm in case of inner race and outer race fault type, whereas 0.1 mm depth is measured in case of ball fault. The motor load is set to 0 hp in this experiment and position relative to the load zone in case of outer race defect is centered at 06:00 shown in Table 1 and Table 2 respectively. The envelope analysis is used to look for a defect in the outer race. The 6205-SKF bearing's BPFO and related parameters are as follows:

$$BPFO = \left\{ \frac{N}{2} \left[ f_i \left( 1 - \frac{d \cos \alpha}{PD} \right) \right] \right\}$$

Where the  $N=09$ ,  $PD = 46.4 \text{ mm}$ ,  $d = 7.2 \text{ mm}$ ,  $\alpha = 0 \text{ degree}$ , inside diameter of bearing = 25mm, and outside diameter of bearing = 52 mm. In the experimental investigation, the sampling frequency and overall data point are 12000 Hz and 122136, respectively.  $f_i = 28.83 \text{ Hz}$  is the shaft frequency. As a result of the aforementioned calculation, the corresponding BPFO, according to the bearing's specifications, is 103.3223 Hz.

For the outer race fault, repeat the process for locating the BPFO and its harmonic. When there is a lot of background noise, it can be difficult to concentrate. As seen in fig. 1, normal bearing and outer race data do not display consistent peaks at BPFI and BPFO Harmonics (6). When a signal is surrounded by a lot of noise, envelope spectrum analysis has great difficulty extracting the frequency of the fault features. In this case, the kurtosis of the vibration data is determined, which shows the impulsiveness of the signal. The kurtosis

value for different forms of bearing faults is shown in Figure 7.

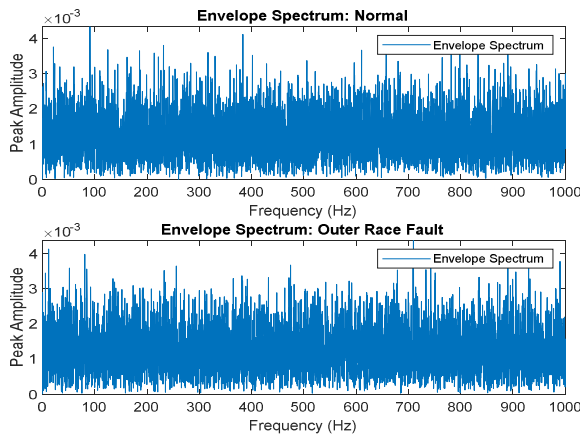


Fig. 7. Envelope spectrum Normal and Outer race (Heavy Background Noise Signals).

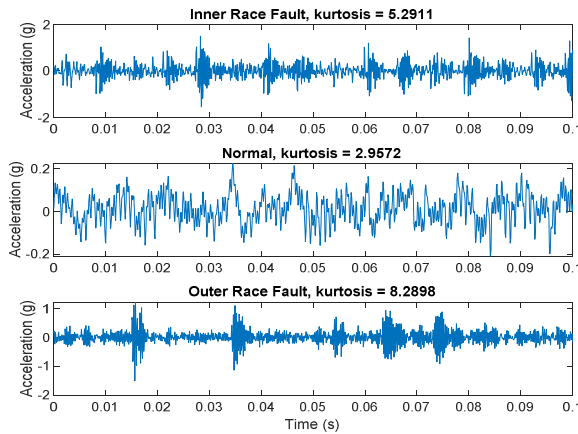


Fig. 8. Time Domain waveform and Kurtosis value of bearing. (a) Inner race, (b) Normal and (c) Outer race.

As seen in fig. 1, the IR defect signal has a higher impulsiveness (3). As a result, the envelope spectrum preserved and visualized the peaks and harmonics at a high level (BPFI). In the case of an OR defect, the peaks at BPFO and its harmonics are mildly noticeable when absorbed in intense background noise. Prior to envelope spectrum review, the impulsive signal should be extracted or the SNR should be amplified (Signal to Noise Ratio). This strong background noise problem is solved by adding Kurtogram [16] as a pre-filter phase and spectrum kurtosis before envelope spectrum analysis.

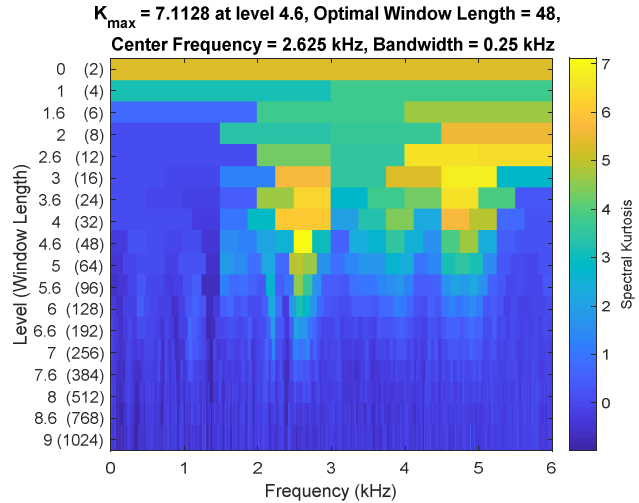


Fig. 9. Kurtogram for Band selection.

It is apparent from fig (7) that immersed noise suppressed the fault function frequency at BPFI and BPFO, implying that no clear pic can be seen in fig(7) for BPFI and BPFO. The time domain waveform and kurtosis value of a bearing with an IR defect, an OR defect, and a regular bearing are shown in Figure 8. The kurtosis of a regular bearing is 2.9572, that of an inner race fault is 5.2911, and that of an outer race fault is 8.2898. As a result, when bearing faulting an inner and outer race, a higher kurtosis value is observed. Higher kurtosis indicates that the signal is non-stationary and is surrounded by a lot of noise. The parameter shown in fig (9) provides the details needed to choose the appropriate bandpass filtering. The bandpass filter is used to pre-filter the data and increase non-stationary portion separation. Maximum kurtosis = 7.1128 at a stage of 4.6, optimum window duration = 48, centre frequency = 2.625 kHz, and bandwidth =0.25 kHz, as seen in fig (8). Kurtogram and spectral kurtosis are used to compute kurtosis locally within a frequency range. After determining the maximum kurtosisvalue-from fig (9)-and its particular frequency band, the bandpass filter was applied to the initial signal to increase its impulsiveness for envelope spectrum analysis. The optimal window length, as described in the kurtogram, is

used to calculate spectral kurtosis, as seen in fig (10). A high spectral kurtosis value often indicates a large power variance (dB) at the corresponding frequency. These higher impulsive data are subjected to envelope spectrum analysis. As a result, a spectral kurtogram is used to locate the non-stationary component of the vibration signal.

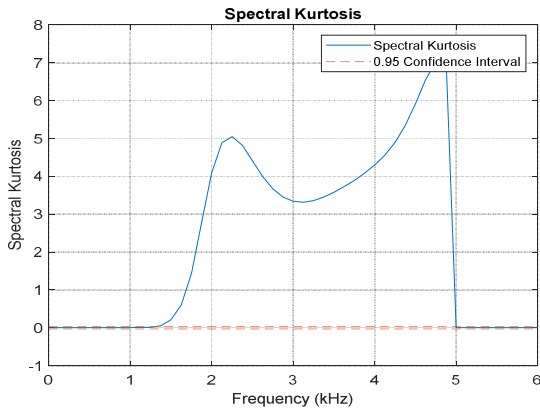


Fig. 10. Spectral Kurtosis

The kurtosis values of the outer race raw signal fault are compared to the kurtosis values of the bandpass filtered outer race raw signal fault in Figure 11. The kurtosis value before bandpass filtering is 8.2898; after bandpass filtering, the kurtosis value is 12.0876. As seen in fig. 10, the higher kurtosis obtained after bandpass filtering is clearly seen.

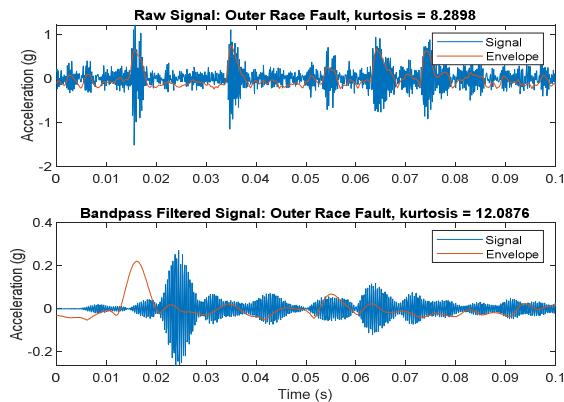


Fig. 11. Band pass filter

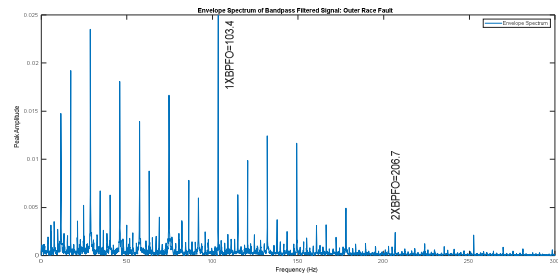


FIG. 12. BANDPASS FILTERED SIGNAL ENVELOPE SPECTRUM WITH ORDEFECT.

The middle frequency ( $f_c$ ) and bandwidth ( $bw$ ) for bandpass filtering were recommended by the kurtogram diagram shown in fig (9). The value of kurtosis is increased by adding bandpass filtering to the original signal data, as seen in fig (10). The modulated peak amplitude of the outer race defect will regain and increase as a result of this. Finally, the envelope signal (shown in fig. 12) is derived, which reflects the measured value of BPFO=103.4 Hz and its harmonics (206.7 Hz). The REB has an outer race flaw, as shown by the observed value of BPFO and its harmonics matching the measured value. Improved envelope spectrum after bandpass filtering with the frequency band submitted by kurtogram and spectral kurtosis. As a result, we look at the outer race defect in the bearing envelope signal, which may indicate a defect at BPFO and its harmonics.

## CONCLUSION

The use of spectral kurtosis in the detection of REB defects is a fascinating new technique. The rolling aspect bearing fault is investigated in this paper at two locations: the inner and outer races. To begin, envelope spectrum analysis is used to determine the frequency of inner race defects and their harmonics. The frequency envelope signal for the inner race defect has a high impulsiveness. As a result, the envelope continuum effectively absorbs the peaks and harmonics at BPFI. Second, the envelope range failed to display any peaks at BPFO and its harmonics for data from the outer race with heavy noise or hardly discernible. In this case, extracting the impulsive signal or amplifying the

SNR is needed before investigating the envelope spectrum (Signal to Noise Ratio). Until performing envelope spectrum analysis, introduce Kurtogram as a pre-filter method and spectrum kurtosis. The problem of a strong noise noisy signal can be overcome by following the steps above. The result confirms that the proposed fault investigation protocol is practical and useful for rolling aspect bearing state monitoring. Furthermore, the experimental investigation described here is characterized by a consistent tempo. Future research will look at the robustness of the proposed solution in the case of rotation speed variations, as well as whether the empirical mode decomposition (EMD) process can be used for non-stationary signals.

## REFERENCES

- [1] S. Zhao, L. Liang, G. Xu, and J. Wang, "Quantitative diagnosis of a spall-like fault of a rolling element bearing by empirical mode decomposition and the approximate entropy method," *Mech. Syst. Signal Process.*, pp. 1–24, 2013.
- [2] P. Agrawal, "Diagnosis and Classifications of Bearing Faults Using Artificial Neural Network and Support Vector Machine," *J. Inst. Eng. Ser. C*, 2019.
- [3] P. Jayaswal, A. K. Wadhvani, and K. B. Mulchandani, "Machine Fault Signature Analysis," *Int. J. Rotating Mach.*, vol. 2008, pp. 1–10, 2008.
- [4] I. El-thalji and E. Jantunen, "A summary of fault modelling and predictive health monitoring of rolling element bearings," *Mech. Syst. Signal Process.*, pp. 1–21, 2015.
- [5] G. Yang, X. Sun, M. Zhang, X. Li, and X. Liu, "Study on Ways to Restrain End Effect of Hilbert-Huang Transform," 2014.
- [6] D. L. Donoho, "De-Noising by Soft-Thresholding," vol. 41, no. 3, 1995.
- [7] N. E. Huang, Z. Wu, S. R. Long, K. C. Arnold, X. Chen, and K. Blank, "On instantaneous frequency," vol. 1, no. 2, pp. 177–229, 2009.
- [8] X. Qin, Q. Li, X. Dong, and S. Lv, "The Fault Diagnosis of Rolling Bearing Based on Ensemble Empirical Mode Decomposition and Random Forest," vol. 2017, 2017.
- [9] J. Xiang and Y. Zhong, "Microelectronics Reliability A fault detection strategy using the enhancement ensemble empirical mode decomposition and random decrement technique," 2017.
- [10] N. Wang and X. Liu, "Bearing Fault Diagnosis Method Based on Hilbert Envelope Demodulation Analysis Bearing Fault Diagnosis Method Based on Hilbert Envelope Demodulation Analysis," 2018.
- [11] D. Hochmann and E. Bechhoefer, "Envelope Bearing Analysis : Theory and Practice  $\Omega$ ," no. August, 2016.
- [12] V. Vrabie and P. Granjon, "Application of spectral kurtosis to bearing fault detection in induction motors," no. January, 2004.